Proceedings of the 28th IEEE
EMBS Annual International Conference
New York City, USA, Aug 30-Sept 3, 2006

Automated Pericardial Fat Quantification in CT Data

Alok N. Bandekar, Morteza Naghavi and Ioannis A. Kakadiaris

Abstract— **Recent evidence indicates that pericardial fat may be a significant cardiovascular risk factor. Although pericardial fat is routinely imaged during Computed Tomography (CT) for coronary calcium scoring, it is currently ignored in the analysis of CT images. The primary reason for this is the absence of a tool capable of automatic quantification of pericardial fat. Recent studies on pericardial fat imaging were limited to manually outlined regions-of-interest and preset fat attenuation thresholds, which are subject to inter-observer and inter-scan variability. In this paper, we present a method for automatic pericardial fat burden quantification and classification. We evaluate the performance of our method using data from 23 subjects with very encouraging results.**

I. Introduction

A recent survey reveals that over 64% of Americans are overweight or obese [1]. Obesity increases the risk for high blood cholesterol, high blood pressure, and diabetes. Individual cardiovascular risk can be quantified by the Framingham Risk Score [2], which integrates age, gender, total and HDL cholesterol, and systolic blood pressure. In modern medicine, fat tissue is no longer viewed as a simple energy storehouse of the body; instead it is considered an active organ with critical metabolic and immune regulatory functions. Recent evidence also indicates that pericardial fat may be a significant cardiovascular risk factor [3], [4]. Taguchi *et al.* have reported that pericardial fat was the strongest independent predictor for hemodynamically significant coronary artery disease (CAD) [3]. Wheeler *et al.* reported that pericardial fat is highly correlated with visceral fat, suggesting that increased pericardial fat, like increased abdominal visceral fat, may be a significant index of risk for CAD [4].

Noninvasive imaging techniques provide minimal-risk opportunities to detect disease, assess the individual risk of patients, and to study patients serially over time in assessment of therapy. Standard noninvasive diagnostic imaging modalities to assess the heart include CT, Single Photon Emission Computed Tomography (SPECT), Positron Emission Tomography (PET), and Magnetic Resonance Imaging (MRI). CT and MRI are both popular imaging modalities used to quantify fat distribution. However, CT is less expensive and provides better contrast between fat and non-fat tissues. In current clinical practice, pericardial fat quantification studies were limited to manually outlined region of interest (ROI) and preset fat attenuation thresholds, which are subject to inter-observer and inter-scan variability. Thus, the development of a computer-assisted method which provides unbiased and consistent results automatically with minimal human intervention is highly desirable.

In our previous work [5], [6], we have developed a tissue segmentation method based on a hierarchical, multi-class, multi-feature, fuzzy affinity framework and applied it for automatic segmentation and quantification of abdominal fat in CT (Automatic Fat Analysis in Computed Tomography - AFACT). In this paper, we extend the framework for automatic pericardial fat quantification.

The rest of the paper is organized as follows. Section II describes in detail the steps of our method. In Section III, we present results from our method and a comparison with manual segmentations, while in Section IV we present our conclusions.

Alok N. Bandekar and Ioannis A. Kakadiaris are with the Computational Biomedicine Lab (formerly known as Visual Computing Lab), Department of Computer Science, University of Houston, Texas 77204, USA abandekar@uh.edu, ioannisk@uh.edu

Morteza Naghavi is with the Association for Eradication of Heart Attack (AEHA), Houston, Texas 77005, USA

II. Materials and Methods

Our work is based on a hierarchical, multi-class, multi-feature, fuzzy affinity-based framework [5], which combines the intensity and texture information with local "hanging togetherness" within a fat class. The fuzzy connectedness constraint for the object extraction presented in [7], [8], [9] is relaxed to allow global segmentation. Thus, instead of applying a space-invariant global threshold value, our computational framework adapts the threshold value locally to account for the local "hanging togetherness" of the tissue to be segmented. The Mahalanobis metric is used to compute the similarity of pixels in the intensity- and texture-based feature space. The most discriminating combination of texture features for specific object regions (fat, nonfat, and background classes) is determined in the training phase of our framework.

A. Experimental Data

We evaluated our method using data from 23 subjects (15 male, 8 female, mean age 54.9±8.8 years). For each, 30 to 35 contiguous transverse images were obtained from the inferior margin of the right pulmonary arterial level (approximately 10 mm superior to the left main coronary artery) to the bottom of the heart. A section thickness of 3 mm, a field of view of 30 cm, and a matrix of 512 x 512 were used to reconstruct the raw image data, yielding a pixel size of 0.59 x 0.59 mm^2 and a voxel volume of 1.0 mm^3.

B. AFACT Algorithm Overview (Pericardial)

I. Training Phase

A. Estimate object-specific (fat, non-fat, background classes) distributions using a training data set.

Step 1: Compute relevant intensity and texture features.

Step 2: Compute the most discriminating features.

II. Deployment Phase

B. Remove artifacts and find the contour outline of the human body.
Step 3: Remove equipment-related artifacts.
Step 4: Find the outline of the human body automatically for processing the data inside this contour.

C. Segment and label various organs/tissues in cardiac scan.
Step 5: Use anatomical landmark information to locate the upper and lower limits of the heart.
Step 6: Segment the inner-thoracic cavity using radial gradient sampling in each slice.
Step 7: Segment the lungs in each slice.
Step 8: Segment the heart and descending aorta in each slice.
Step 9: Update the 3D label map of the various organs in the volume.

D. Compute the fat statistics using the sample area around the seed point.
Step 10: Compute a seed point for the fat region in the center slice.
Step 11: Compute statistics dynamically for a sample region around the seed point.

E. Compute the fuzzy affinity-based object.
Step 12: Compute the most discriminating features selected from Step 2.
Step 13: Compute the global object affinity using the Mahalanobis metric.
Step 14: Compute the fat by thresholding the global object affinity image.
Step 15: Use labels determined in step 9 to quantify pericardial fat.

C. AFACT Algorithm Description (Pericardial)

1) Steps 1-2, Training Phase: Initially, Laws' features [10] and Gabor texture features [11] for the cardiac CT images were computed. The most discriminating feature combinations were determined according to their cumulative discriminating power. Our feature vector consisted of two features, namely intensity and Laws' ss feature.

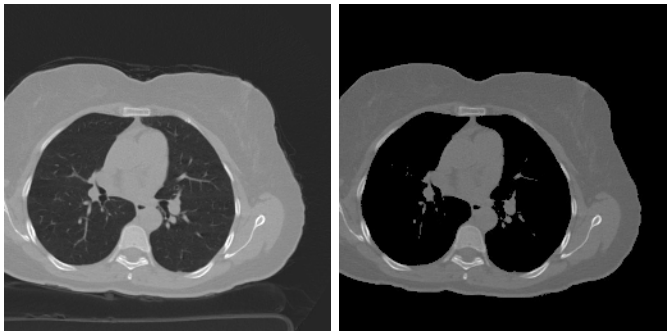

(a) (b)

Fig. 1. Removal of equipment-related artifacts: (a) original CT image, and (b) after artifact (e.g., table, wire) removal.

2) Step 3, Remove equipment-related artifacts: Many artifacts in the CT image (e.g., the patient table and wires) have intensity distributions very similar to that of the fat tissue. To correctly quantify the fat burden, it is important that such artifacts are removed from the image. We perform an artifact removal preprocessing step that automatically removes such artifacts. More details can be found in [6]. Figure 1(b) depicts the image after the removal of detected equipment-related artifacts.

3) Step 4, Find the outline of the human body contour: First, we threshold the preprocessed image obtained after artifact removal step within the interval $(-190 < Hu < -30)$, a normal attenuation range for fat tissues [12]. Then, we perform outer boundary detection by looking at the intensity profile of equi-angular radial vectors originating from the centroid of the thresholded image. We call this method radial sampling, where each of these radial vectors is traversed with a first order gradient filter kernel to mark the points where there is a change from background to ROI. The outermost points on these vectors are marked as points on the human boundary contour. Figure 2(b) depicts the filled human body contour after the outline is detected.

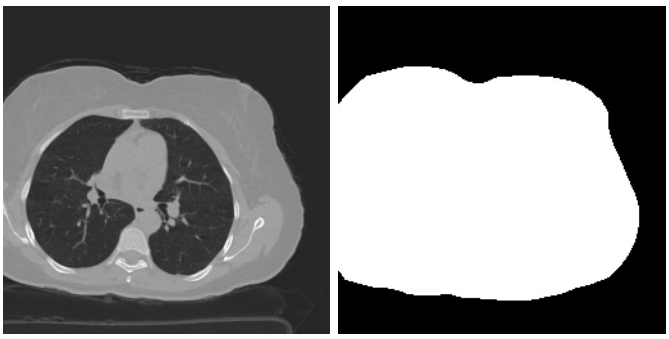

(a) (b)

Fig. 2. Human body contour detection: (a) original CT image, and (b) filled human contour.

4) Steps 5-9, Segment and label various organs/tissues in cardiac scan: We consider slices between the start and end of the heart using anatomical landmark information. Specifically, we use the splitting of the pulmonary artery landmark slice to mark the start of the heart and the 2-3 slices below the appearance of the liver to mark the end of the heart. We use the area enclosed by the human body contour as our ROI and only search for fat pixels inside it. We locate the inner-thoracic cavity contour by using radial sampling as described in Step 3. Figures 3(a-b) depict the contours obtained by the radial sampling method. In addition to the fat threshold, we use a bone threshold (130 HU) in order to mark the points at the spinal cord. The use of a fat threshold alone does not produce clear boundaries around the spinal cord. After we obtain the inner contour, which is also the boundary of the lungs, we label the region between the human contour and the lung boundary as subcutaneous thoracic region. Now the tissues inside the inner contour are fat, heart, and lung. The distribution of the lung tissue is well

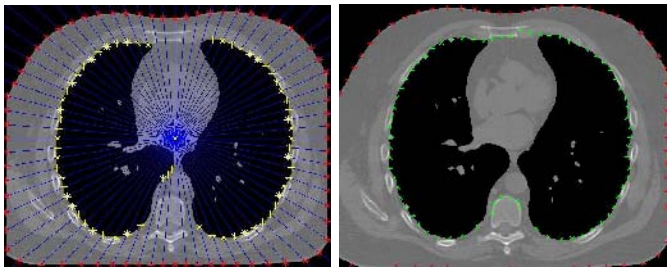

(a) (b)

Fig. 3. Inner-thoracic cavity segmentation: (a) Radial sampling method, and (b) refined contour.

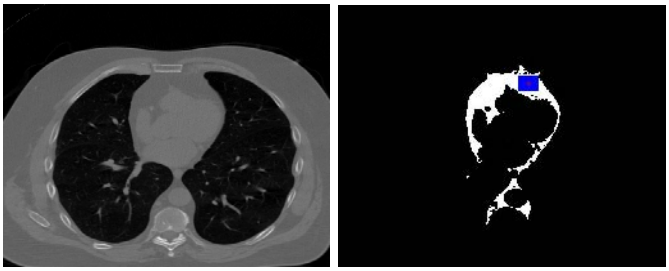

(a) (b)

Fig. 5. Dynamic computation of fat statistics: (a) Original image, and (b) sample region in the fat tissue.

separated from the distribution of the heart and fat tissues in the histogram of the image. We compute a dynamic threshold to segment the lungs and assign a label. After the lung tissue has been removed, only the heart and fat tissues are left in the ROI. We take a sample pixel at the center of the ROI to compute the statistics of heart and threshold it with mean $\pm$ 2std to segment the heart tissue and apply a label to it. At the starting slice of the heart, we perform circle detection using the Hough transform to detect the descending aorta and track this circle in the following slides. Thus, we have labelled background, subcutaneous region, lungs, heart, and descending aorta in the 3D cardiac scan. Figure 4(b) depicts the label map for various organs/tissues.

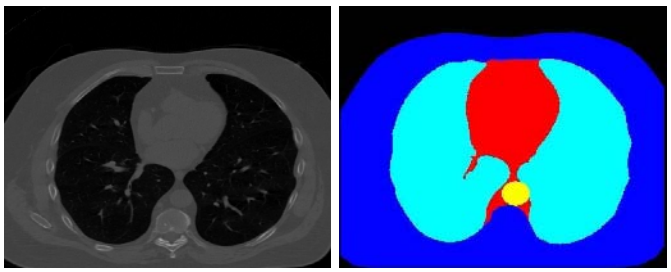

(a) (b)

Fig. 4. Label Map: (a) Original image, and (b) corresponding labeled image.

5) Steps 10-11, Compute the fat statistics dynamically: We compute the statistics for fat tissue in only one slice (i.e., the center slice of the cardiac scan). In step 8, after we threshold for heart tissue, most of the remaining tissue is the fat tissue which is not a contiguous region. We fit a square of maximum allowable size and compute dynamic statistics of fat by taking samples around the center of the square. Figure 5b depicts the sample region around the seed point for computation of fat statistics. The average Hu for fat tissue varies across subjects and also depends on the CT scanner [12]. We use these dynamically computed fat statistics in our fuzzy affinity computation to make the method scanner independent.

6) Steps 6-8, Compute the fuzzy affinity-based object: First, the most discriminant features selected from Step 2 of the training phase are computed for the current image. Then, the global object affinity is computed using the Mahalanobis metric. The global affinity image has values between 0 and 1; the higher the value, the higher the probability that the tissue belongs to the fat region. The fat areas are obtained by thresholding the global object affinity image and using the global label map obtained from Step 9.

III. Results and Discussion

We have compared the results of our method to expert manual segmentations of pericardial fat for 23 subjects. The manual delineation of the fat region in the CT images, performed by experienced physicians/radiologists, was used as the gold standard. We evaluated the results of our algorithm by computing the three measures of accuracy recommended by Udupa *et al.* [13]. Specifically, we computed the false negatives, false positives, true negatives, and true positives by computing the number of pixels that were classified as the background and the ROI, both correctly and incorrectly.

Figures 6(a-c) depict the accuracy, the true positive rate, and the true negative rate obtained by AFACT for pericardial fat quantification when compared with manual segmentation respectively. The mean accuracy for pericardial fat was $99.13\% \pm 0.38\%$. The mean true negative rate was $99.28\% \pm 0.33\%$. Finally, the mean true positive rate was found to be $85.63\% \pm 7.42\%$. The qualitative results of our algorithm for a subject at the split of the Left Main (LM), 2 slices above the LM, and 3 slices below the LM are depicted in Fig. 7.

IV. Conclusions

In this paper, we have presented a method for automatic pericardial fat quantification. We have successfully quantified and classified the pericardial fat burden in cardiac CT images and performed evaluation against manual segmentations by experts. Our method achieves a comparable true negative rate and accuracy versus manual delineation of pericardial fat. This technique does not require seed initialization, correlates very well with manual readings by humans, and requires slightly less than one minute per CT slice. Clinical investigation of this tool is warranted to evaluate the role of pericardial fat in risk assessment.

References

[1] K. Flegal, M. Carroll, C. Ogden, and C. Johnson, "Prevalence and trends in obesity among US adults,1999-2000," *Journal of the American Medical Association*, vol. 288, pp. 1723–7, 2002.

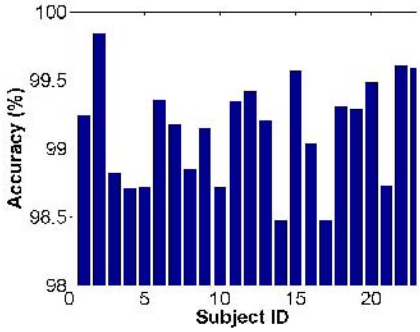

(a)

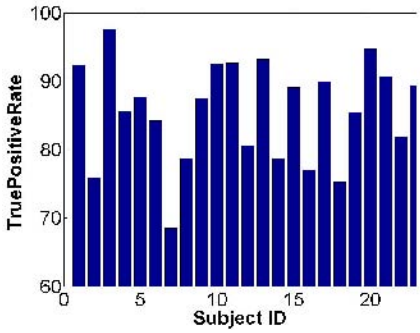

(b)

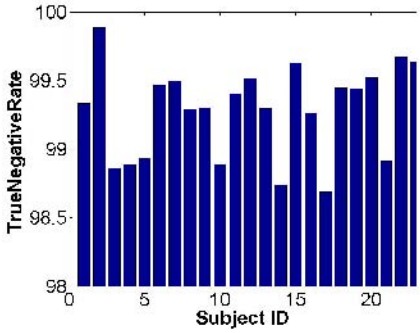

(c)

Fig. 6. Performance evaluation of AFACT for total fat segmentation: (a) accuracy, (b) true positive rate, and (c) true negative rate.

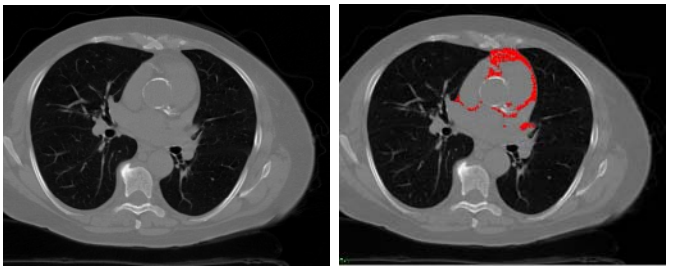

(a) (b)

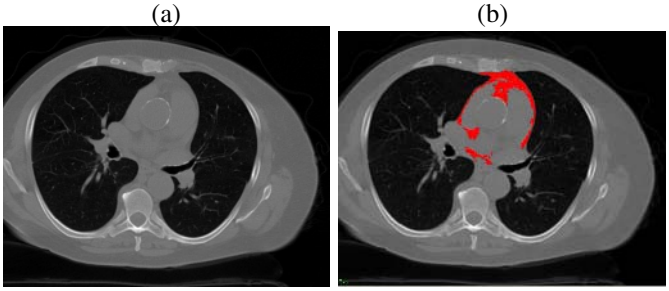

(c) (d)

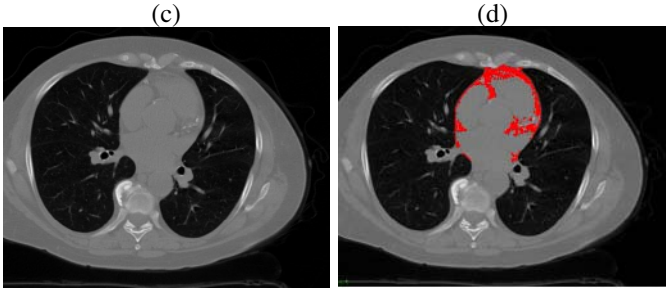

(e) (f)

Fig. 7. Pericardial fat measured at left main (LM) artery split, 2 slices below LM level, and 3 slices below LM: (a,c,e) Original images, and (b,d,f) estimated pericardial fat (overlaid in red) respectively.

[2] P. W. Wilson, R. B. D'Agostino, D. Levy, A. M. Belanger, H. Silbershatz, and W. B. Kannel, "Prediction of coronary heart disease using risk factor categories," *Circulation*, vol. 97, pp. 1837–47, 1998.

[3] R. Taguchi, J. Takasu, Y. Itani, R. Yamamoto, K. Yokoyama, S. Watanabe, and Y. Masuda, "Pericardial fat accumulation in men as a risk factor for coronary artery disease," *Atherosclerosis*, vol. 157, no. 1, pp. 203–9, 2001.

[4] G. L. Wheeler, R. Shi, S. R. Beck, C. D. Langefeld, L. Lenchik, L. E. Wagenknecht, B. I. Freedman, S. S. Rich, D. W. Bowden, M. Y. Chen, and J. J. Carr, "Pericardial and visceral adipose tissues measured volumetrically with computed tomography are highly associated in type 2 diabetic families," *Invest Radiology*, vol. 40, pp. 97–101, 2005.

[5] A. Pednekar, A. N. Bandekar, I. A. Kakadiaris, and M. Naghavi., "Automatic segmentation of abdominal fat from CT data," in *Proceedings of the 7th IEEE Workshops on Application of Computer Vision (WACV/MOTION'05)*, Colorado, USA, January 5-7 2005, pp. 308–315.

[6] A. N. Bandekar, M. Naghavi, and I. A. Kakadiaris., "Performance evaluation of abdominal fat burden quantification in CT," in *Proceedings of the 27th Annual International Conference of the IEEE Engineering in Medicine and Biology Society*, Shanghai, China, September 1-4 2005.

[7] A. Pednekar and I. Kakadiaris, "Image segmentation based on fuzzy connectedness using dynamic weights," *IEEE Transactions in Image Processing*, vol. 15, no. 6, pp. 1555– 1562, June 2006.

[8] A. Pednekar, U. Kurkure, I. Kakadiaris, R. Muthupillai, and S. D. Flamm., "Left ventricular segmentation in MR using hierarchical multi-class multi-feature fuzzy connectedness," in *Proceedings of the 7th International Conference on Medical Image Computing and Computer-Assisted Intervention*, Saint-Malo, France, September 26-30 2004, pp. 402–410.

[9] J. Udupa and S. Samarasekera, "Fuzzy connectedness and object definition: theory, algorithms, and applications in image segmentation," *Graphical Models and Image Processing*, vol. 58, no. 3, pp. 246–261, May 1996.

[10] K. Laws, "Texture image segmentation," Ph.D. dissertation, University of Southern California, 1980.

[11] B. Manjunath and W. Ma, "Texture features for browsing and retrieval of image data," *IEEE Transactions on Pattern Analysis and Machine Intelligence*, vol. 18, no. 8, pp. 837–842, August 1996.

[12] Y. Tohru, N. Tadashi, Y. Mitsukazu, H. Abdul, M. Masakazu, Y. Kouichi, A. Takeshi, K. Kazuaki, F. Tohru, Y. Shizuya, and M. Yuji, "Abdominal fat: Standardized technique for measurement at CT," *Radiology*, vol. 211, pp. 283–286, 1999.

[13] J. Udupa, Y. Jin, C. Imielinska, A. Laine, W. Shen, and S. Heymsfield, "Segmentation and evaluation of adipose tissue from whole body MRI scans," in *Proceedings of the 6th International Conference on Medical Image Computing and Computer-Assisted Intervention*, Montreal, Canada, November 15-18 2003, pp. 635–642.